Fachtagung “Experimentelle Strömungsmechanik”
7.–9. September 2021, Bremen

Vergleich zwischen sensorbasierten Druckmessungen und „Pressure from PIV“ für unterschiedliche Strömungsbedingungen

A comparison between sensor based pressure data and "Pressure from PIV" for multiple flow conditions

Timo Gericke, Steffen Hüttig, Juan Camilo Londono Alfaro, Yunus Üstüner
Volkswagen AG, Wolfsburg

PIV, Druckfelder; Pressure from PIV, Stumpfkörper, Nachlauf
PIV, Pressure field; Pressure from PIV, Bluff Body, Wake

Abstract

In this work a comparison between pressure determined from advanced 3D Lagrangian Particle Tracking (LPT) using the Shake-The-Box (STB) method and static pressure taps measurements in a low-speed flow regime is presented. LPT offers the possibility to acquire a field of pressure instead of pointwise measurements. This is an advantage especially for novel aerodynamic and aeroacoustic analysis otherwise only possible with expensive and time consuming instrumentation of the model. Results of the LPT-based pressure reconstruction are compared with static pressure taps on the surface of a solid rib and a cube installed on a flat plate. The aim of this study is to assess if LPT may be considered as a complementary method to pressure taps, or even as a possible replacement. Therefore, the flow field is measured with a volumetric multi-camera setup. Multiple methods may be used to obtain the averaged pressure fields from PIV and LPT measurements. In this study *LaVision's* state-of-the-art software package "Pressure from PIV" is used, which uses the Reynolds-averaged Navier-Stokes (RANS) equation to calculate the time-averaged pressure field. A spatiotemporal resolution can be achieved by a pseudo Lagrangian fluid trajectory based on the LPT and a polynomial approximation. It will be shown that although the areas with low and high pressure are being detected, a deviation is always visible especially in regions with a relatively low particle image density. The Reynolds number based on the height is 25500 and 38000.

Introduction

Fluid pressure measurements are crucial for deeper insights into the physics of aerodynamics, aeroacoustics and fluid-structure interactions. Typically, fluid pressure is measured pointwise with static pressure taps or pitot tubes (Tropea et al. 2007). These methods lead to reliable results and are therefore widely approved. Nevertheless, pointwise pressure measurements have some drawbacks. Pointwise pressure measurements suffer from low spatial resolution. In industrial applications, the number of surface pressure taps can easily grow to hundreds or thousands which lead to a massive increase in complexity. Implementation is time consuming, expensive and not always possible. Parts which are crucial for the safety of an experimental model and thin and flexible surfaces (Jux et al. 2019) are examples, where an implementation of surface pressure taps is not possible. Moreover, the location and spacing of the static pres-

sure taps must be specified before the manufacturing process. A later adjustment is not possible and therefore an a-priori knowledge of the flow topology is fundamental for a smart placement of the pressure taps. Particle image velocimetry (PIV) and Lagrangian Particle Tracking (LPT) are promising techniques to overcome these drawbacks. Due to recent improvements of PIV/LPT and in the field of post-processing techniques it is nowadays possible to measure the flow pressure in a non-intrusive way with high resolution together with the flow field (van Oudheusden 2013; Gent et al. 2017, Tagliabue et al. 2017, Van der Kindere et al. 2019). For industrial applications volumetric PIV/LPT techniques with sufficient optical access are mandatory. Especially robotic volumetric PIV/LPT are very promising tools for measurements on an industrial scale (Jux et al. 2018a).
Over the last years different methods for estimating pressure from PIV/LPT were developed. Here, the main differences between the approaches lies in the way the pressure gradients are determined using the Navier-Stokes equation. The four main approaches are Reynolds-averaging- (van Oudheusden et al. 2007), Eulerian- (Kat and van Oudheusden 2012), pseudo-Lagrangian- (Kat and van Oudheusden 2012) and Taylor's hypothesis approach (Kat and Ganapathisubramani 2012). A detailed overview is given in Van der Kindere et al. (2019).

The objective of this study is to compare sensor based surface pressure data with pressure determined using *LaVision's* state-of-the-art software package "Pressure from PIV" for multiple flow conditions. This software package is based on the Reynolds-averaged Navier-Stokes equation as described by van Oudheusden (2013). Using the momentum equation for an incompressible flow the pressure gradient can be calculated by:

$$\nabla p = -\rho \frac{D\boldsymbol{u}}{Dt} + \mu \nabla^2 \boldsymbol{u}. \quad (1)$$

The expression $\frac{D\boldsymbol{u}}{Dt}$ is the material acceleration, which in the case of a PIV/LPT measurement is the instantaneous fluid particle acceleration. If time-resolved information is not available the averaged pressure distribution can be determined from the local velocity gradient as the material acceleration and equation 1 can be rewritten as:

$$\nabla \bar{p} = -\rho\{(\overline{\boldsymbol{u}} \cdot \nabla)\, \overline{\boldsymbol{u}} + \nabla \cdot \overline{\boldsymbol{u}'\boldsymbol{u}'} - \nu \nabla^2 \overline{\boldsymbol{u}}\}. \quad (2)$$

The second step is to calculate the pressure field by a spatial integration of the pressure derivatives. In the case of an averaged pressure field the Poisson equation is to be solved:

$$\nabla^2 \bar{p} = \nabla \cdot (-\rho\{(\overline{\boldsymbol{u}} \cdot \nabla)\, \overline{\boldsymbol{u}} + \nabla \cdot \overline{\boldsymbol{u}'\boldsymbol{u}'} - \nu \nabla^2 \overline{\boldsymbol{u}}\}). \quad (3)$$

To fully close the problem boundary conditions are then needed. Dirichlet boundary conditions (i.e pressure values) can be measured using a Pitot-static tube. Newmann boundary conditions (i.e pressure gradients) can be positioned in the free flow upstream and downstream of the object and on the wall surface.

Depending on the results of the comparison, PIV/LPT will possibly replace pressure taps in future applications giving the advantage that surface pressure and velocity can be determined from a single measurement with high spatial resolution.

Experimental Setup

Experiments presented in this work are conducted in the calibration wind tunnel at the *Volkswagen AG* in Wolfsburg. The facility is an open jet wind tunnel (*Airflow Developments Ltd.*) with a nozzle exit diameter of 152 *mm*. A motor rated power of 1.5 *kW* enables wind speeds between 1 and 30 *m/s*. A flat plate (see Fig. 1) with an elliptical nose (6:1), a length of 800 *mm* and a width of 300 *mm* is centered 150 *mm* after nozzle's exit. On top of the flat plate a solid rib and a cube are mounted separately 300 *mm* and 290 *mm* in streamwise direction (see Fig. 1). All parts of the flat plate and the models have been painted black in order to reduce noise due to reflection of the laser light. Rib height H is 40 *mm* and the width is identical to that of the flat plate. The cube has a height of 60 *mm*. Mean pressure was acquired through 0.8 *mm* circular static pressure taps located in the centerline of the flat plate and on the surface of the solid rib and the cube. Distance between the pressure taps on the flat plate is 0.5H, 0.25H on the rib and 0.25H, 0.5H and 0.75H on the cube. The first tap is located at x/H = 3. Overall 50 and 70 pressure taps were measured using a Scanivalve DSA3217 with 16 channels per module. Free stream velocity was set to 10 *m/s* resulting in a Reynolds number based on the height of Re_H = 25500 and 38000. During the experiment the ambient temperature was 22 *°C*.

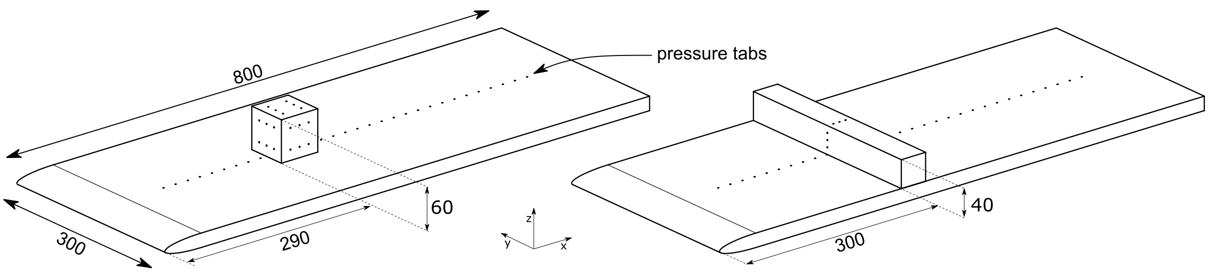

Fig. 1: Sketch of the flat plate with cube (left) and solid rib (right).

For the acquisitions of the recording the MiniShaker Aero system from *LaVision* was used. It exhibits four CCD-Cameras with an double image rate of 100 *Hz* at full resolution of 1920 x 1280 pixels with macro planar lenses (f-number = 4 , f = 12 *mm*). In addition, the Mini-Shaker incorporates lenses for the expansion of the laser. The Nd:YAG laser NanoPIV from Litron with an output energy of 50 *mJ* per pulse at a wavelength of 532 *nm* was connected to the Mini-Shaker through an optical fiber cable. The total measured volume was 300 x 500 x 150 mm^3. Synchronization between the laser and the cameras is assured by a PTU X from *LaVision*. Helium Filled Soap Bubbles (HFSB) were used as tracer particles with a mean size of 300 *µm*. A HFSB generator from *LaVision* was used to generate the seeding particles. The entire set-up is shown exemplarily in Fig. 2.

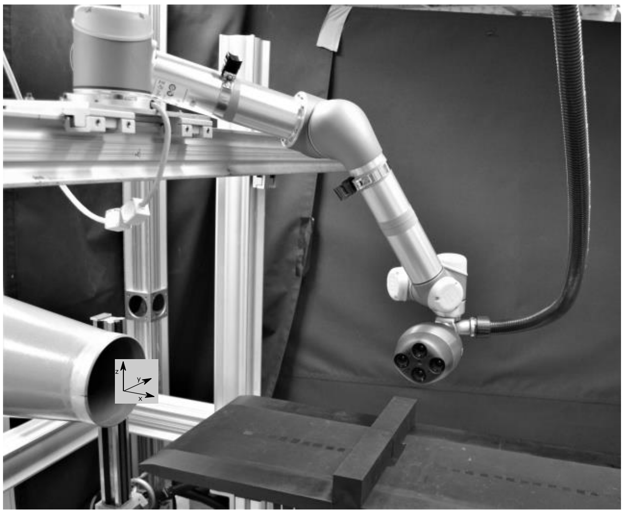

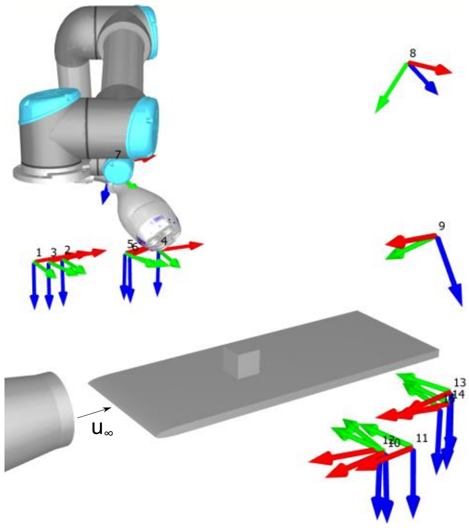

Fig. 2: Experimental setup for the robotic LPT measurements (left) Sketch of the experimental setup showing the robot positions during the measurements (right).

The whole flow fields of the cube and the rib were measured from 15 and 13 different viewing positions, respectively. The camera coordinate systems of those perspectives are shown in Fig. 2. For each data set 500 double-images were recorded with DaVis 10 from *LaVision.*

Results

The following figures provide information of the flow fields around a cube and a rib for a flow velocity of u_∞ = 10 *m/s*. Figure 3 shows the mean velocity profile upstream of the obstacles at y/H = 4. The mean velocity profile compares very well for both geometries.

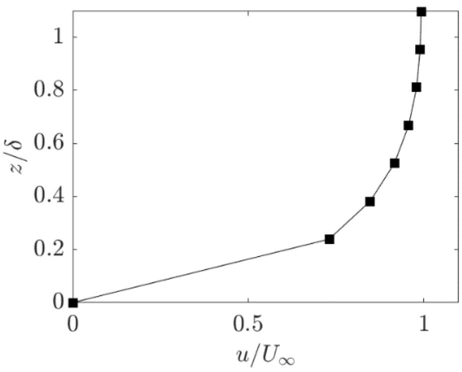

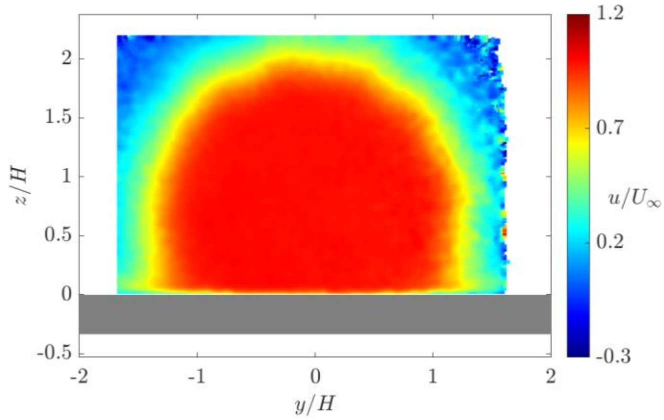

Fig. 3: Mean u-velocity profile upstream of the obstacles (left) Mean u-velocity field (right).

A result of the 3D mean flow, color coded by the stream wise velocity, is given in Fig.4 for the cube and 5 for the rib. In total five and four slices through the volume are shown. Figure 4 shows a much smaller separation region downstream of the cube compared to the one of the rib (Fig. 5). The upstream horseshoe vortex and the separated flows at the corners and on top of the cube can be clearly seen.

GALA e.V., Karlsruhe, Germany, ISBN 978-3-9816764-7-1

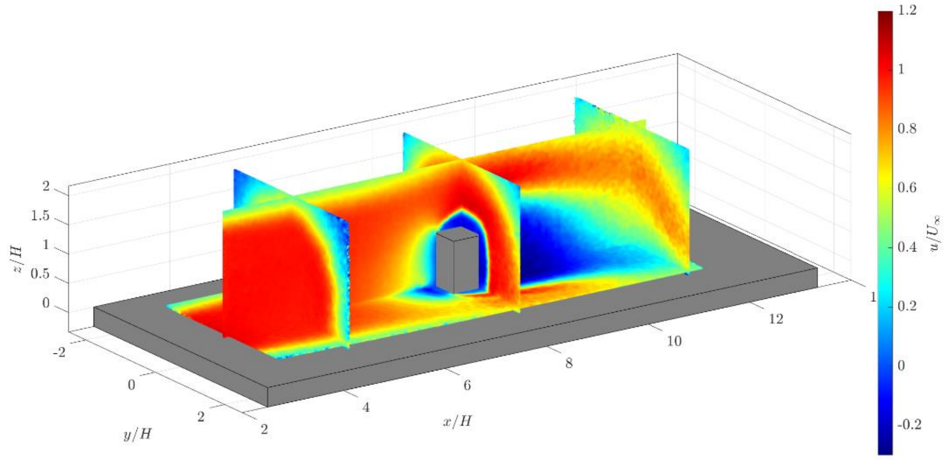

Fig. 4: Bin-averaged u-velocity fields around the cube.

The velocity fields for the rib reveal a large separation region behind the obstacle and a smaller one upstream. These results are very similar to the ones from Van der Kindere et al. (2019) for the smallest rib length.

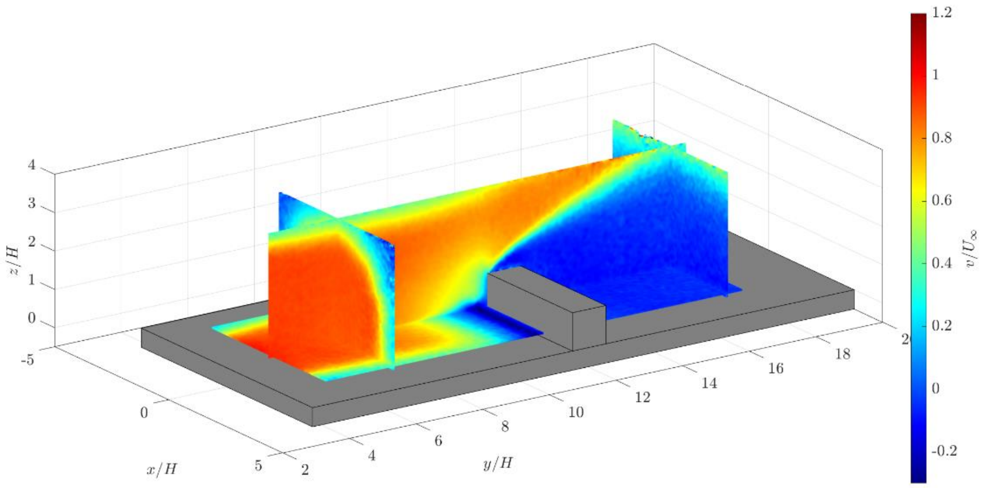

Fig. 5: Bin-averaged u-velocity fields around the rib.

The pressure fields and a direct comparison between sensor based pressure data and “Pressure from PIV” are provided in Fig. 6 and Fig. 7 for the cube and rib, respectively. The used Dirichlet boundary conditions (pressure values from tabs) are shown as black dots.

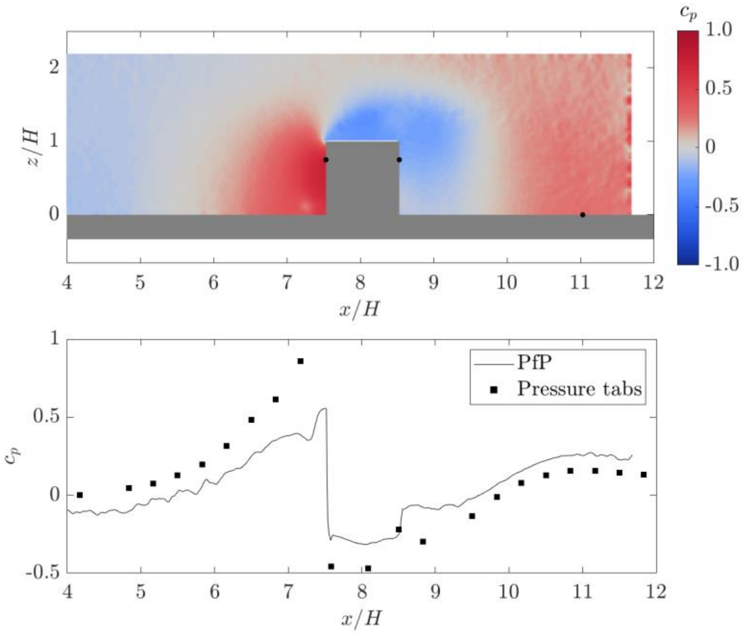

Fig. 6: Bin-averaged pressure field around the cube and pressure coefficient along the symmetry line from the pressure field from PTV/LPT at a height of 4 *mm* over the surface and from the pressure tabs.

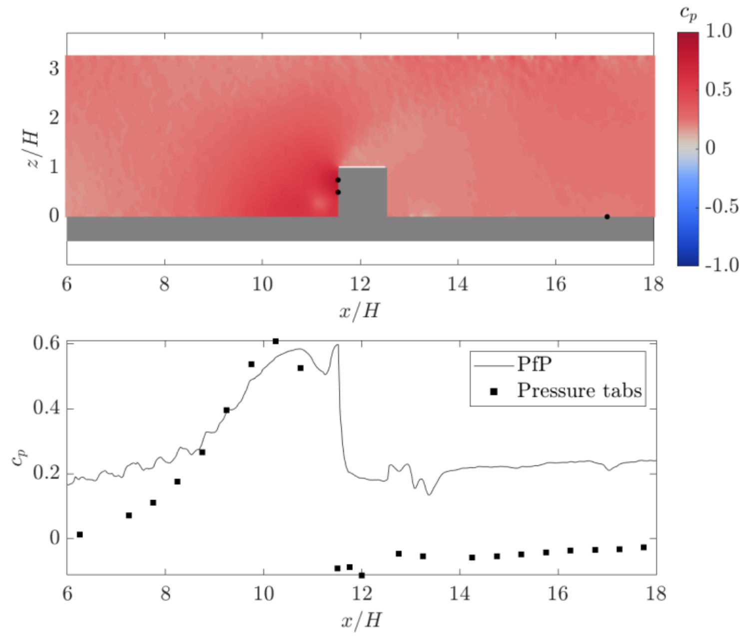

Fig. 7: Bin-averaged pressure field around the rib and pressure coefficient along the symmetry line from the pressure field from PTV/LPT at a height of 4 *mm* over the surface and from the pressure tabs.

The main advantage from PfP can easily be seen in the spatial resolution of the pressure fields. A relative quick and non-intrusive measurement procedure results in a high quantity of pressure data, which with the common procedure using pressure tabs could take weeks or is simply not possible. The quality of the measurements can be determined with the comparison of the pressure coefficient between both measuring techniques. From Fig. 6 can be noted that although the areas with low and high pressure are being detected, a discrepancy is always visible especially in regions with a low particle image density. The largest disparity can be observed in the wake of the rib (Fig. 7).

Conclusion

In this work the pressure information derived from the 3D velocity fields using *LaVision's* software package "Pressure from PIV" was compared to the widely used pressure taps. The velocity fields were acquired using robotic LPT and "Shake-the-Box". For comparison two different obstacles were separately used to evaluate the performance of PfP for different flow conditions, namely a cube and a rib mounted on a plate. The main advantage of deriving the pressure field from the velocity information is the achievable spatial resolution in a relatively time efficient manner, as it can be seen in the results. Nevertheless, a discrepancy between the pressure tabs and the pressure from PfP in absolute values was notable. It can be concluded that the discrepancy increases in regions with low particle image density (e.g. in separated regions) and close to surfaces.
Volumetric masking of the objects is mandatory for the pressure solver of DaVis to prevent unphysical calculation. In future experiments more sub volumes and an increased number of recorded images should be used to compensate the poor particle density in separated regions, in order to align the resulting standard deviation in all measured regions. Moreover, boundary conditions measurement with a static probe in the free stream could enhance the PfP-method and will be used for comparison in future experiments.

The results, opinions and conclusions expressed in this publication are not necessarily those of Volkswagen Aktiengesellschaft.

Acknowledgment

The authors would like to thank Dirk Michaelis and Jeon Jin Young from *LaVision GmbH* for the support during the evaluation of the experiments.

Literature

De Kat, R., & Van Oudheusden, B. W. (2012). Instantaneous planar pressure determination from PIV in turbulent flow. *Experiments in fluids*, *52*(5), 1089-1106.

De Kat, R., & Ganapathisubramani, B. (2012). Pressure from particle image velocimetry for convective flows: a Taylor's hypothesis approach. *Measurement Science and Technology*, *24*(2), 024002.

Jux, C., Sciacchitano, A., Schneiders, J. F., & Scarano, F. (2018). Robotic volumetric PIV of a full-scale cyclist. *Experiments in Fluids*, *59*(4), 1-15.

Jux, C., Scarano, F., & Sciacchitano, A. (2019, July). Aerodynamic pressure reconstruction on generic surfaces from robotic PIV measurements. In *Proceedings of the 13th International Symposium on Particle Image Velocimetry* (pp. 22-27). Universitat der Bundeswehr Munchen.

Tagliabue, A., Scharnowski, S., & Kähler, C. J. (2017). Surface pressure determination: a comparison between PIV-based methods and PSP measurements. *Journal of Visualization*, *20*(3), 581-590.

Tropea, C., & Yarin, A. L. (2007). *Springer handbook of experimental fluid mechanics*. Springer Science & Business Media.

Van Gent, P. L., Michaelis, D., Van Oudheusden, B. W., Weiss, P. É., de Kat, R., Laskari, A., & Schrijer, F. F. J. (2017). Comparative assessment of pressure field reconstructions from particle image velocimetry measurements and Lagrangian particle tracking. *Experiments in Fluids*, *58*(4), 33.

Van der Kindere, J. W., Laskari, A., Ganapathisubramani, B., & De Kat, R. (2019). Pressure from 2D snapshot PIV. *Experiments in fluids*, *60*(2), 32.

Van Oudheusden, B. W., Scarano, F., Roosenboom, E. W., Casimiri, E. W., & Souverein, L. J. (2007). Evaluation of integral forces and pressure fields from planar velocimetry data for incompressible and compressible flows. *Experiments in fluids*, *43*(2), 153-162.

Van Oudheusden, B. W. (2013). PIV-based pressure measurement. *Measurement Science and Technology*, *24*(3), 032001.